Synthesis, Solid-State Structure, and Electronic Nature of a Phosphinine-Stabilized *triangulo* Palladium Cluster

Manfred T. Reetz,*[a] Edward Bohres,[a] Richard Goddard,[a] Max C. Holthausen,[b] and Walter Thiel*[b]

Abstract: The reaction of $Pd(OAc)_2$ with an excess of 2,4,6-triphenylphosphinine results in the formation of a red dimeric Pd^0 complex of unknown structure. Treatment of this complex with PEt_3 affords a novel green *triangulo* Pd_3 cluster that is stabilized by three phosphinine and three PEt_3 ligands. An X-ray structural analysis shows that the phosphinine ligands serve as bridges between two Pd atoms. Quantum-mechanical calculations of a model compound reproduce the experimental geometry of the real complex adequately and also illuminate the bonding properties. Specifically, the interaction energy between each phosphinine ligand and the Pd_3 core amounts to 42.2 kcal mol^{-1} and involves both σ and π orbitals.

Keywords: cluster compounds · density functional calculations · MO interactions · P ligands · palladium

Introduction

Many different types of structurally well-defined transition metal clusters have been described in the literature,[1] including a number of homonuclear *triangulo* metal complexes. Such compounds can occur in the anionic, cationic, or neutral form, depending upon the nature of the metal, the oxidation state, and the type of stabilizing ligand. Generally, the electronic nature and bonding properties of metal clusters are fairly well understood,[1, 2] although ambiguities arise from time to time.

Carbon monoxide and phosphanes such as PPh_3 are the most common stabilizing ligands in metal cluster chemistry.[1, 2] In the case of palladium, examples of *triangulo* clusters include $[Pd_3(CO)_3(PPh_3)_3]$,[3] $[Pd_3(CO)_3(PPh_3)_4]$,[3] and $[Pd_3(CN\text{-}c\text{-}C_6H_{11})_6]$.[4] Other types of commonly occurring structural motifs in clusters include main group elements, for example, Cl, S, or PPh_2, which serve as bridges between two metal centers. Examples from Pd chemistry are the trinuclear complexes $[Pd_3Cl(PPh_2)_2(PPh_3)_3][BF_4]$,[5] $[Pd_3Cl(PPh_2)_2(PPh_3)_3]Cl$,[6] $[Pd_3(\mu_2\text{-}SPh)(\mu_2\text{-}PCy_2)_2(PCy_2H)_2(SPh)]$,[7] $[Pd_3(PPh_2)_3(PR_3)_3][BF_4]$,[8] $[Pd_3Cl(PPh_2)_2(PEt_3)_3][BF_4]$,[9] $[Pd_3(PBu_2)_3(CO)_2Cl]$,[10] $[Pd_3(PEt_3)_3(NPh)_2(NHPh)]Cl$,[11] and $[Pd_3(SO_2)_2(CN{-}t\text{Bu})_5]\cdot 2\,C_6H_6$,[12] all of which contain a triangular Pd_3 core.

[a] Prof. Dr. M. T. Reetz, E. Bohres, Dr. R. Goddard
Max-Planck-Institut für Kohlenforschung
Kaiser-Wilhelm-Platz 1, D-45470 Mülheim/Ruhr (Germany)
Fax: (+49) 208-306-2985
E-mail: reetz@mpi-muelheim.mpg.de

[b] Prof. Dr. W. Thiel, Dr. M. C. Holthausen
Organisch-chemisches Institut, Universität Zürich
Winterthurerstrasse 190, CH-8057 Zürich (Switzerland)

In addition to phosphanes (PR_3) and complexes containing PR_2 phosphido bridges, other types of phosphorus compounds such as phosphites, phosphonites, and phosphinites are also known in the general area of transition metal coordination chemistry. Phosphorus-containing heterocycles such as phosphinines (formerly called λ^3-phosphorines or phosphabenzenes) are also capable of forming complexes with transition metal complexes;[13] a $\eta^1(\sigma)$ or a $\eta^6(\pi)$ coordination mode is the most common.[13, 14] Early examples are the chromium complexes **2** and **3**, respectively.[15] In addition, other types of coordination have been reported.[16]

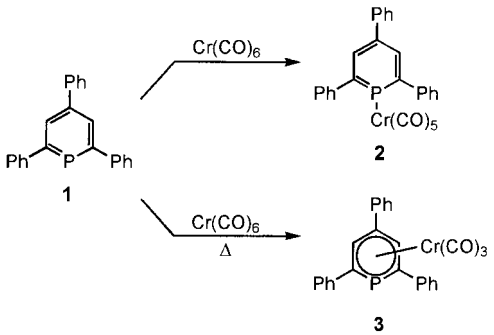

Phosphinines are known to have significant aromatic character; the lowest unoccupied molecular orbital (π*) of the parent compound PC_5H_5 has a relatively high localization at phosphorus that suggests a high π-acceptor capacity.[13, 14] The in-plane lone electron pair corresponds to the third highest occupied level at about −10.0 eV, which can be compared with −10.6 eV known for PH_3. This implies pronounced σ-donor properties.

In the present paper we describe the serendipitous discovery of a novel *triangulo* Pd_3 cluster in which the phosphinine **1**

participates in a purely bridging manner. Detailed quantum-mechanical calculations are included; these illuminate the bonding properties of the complex and the source of stabilization of the Pd_3 core.

Results and Discussion

Synthesis and structure determination: The original goal of our research was the synthesis of a 14-electron Pd^0 complex **5** in which two molecules of the bulky phosphinine **1** serve as the stabilizing ligands.[17] It was envisaged that compound **1**,

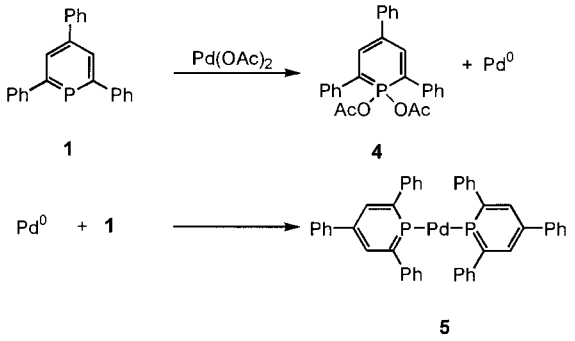

being a well-known reductant in the case of such metal salts as $Hg(OAc)_2$,[13a] could reduce $Pd(OAc)_2$ to the zero valent state and that excess phosphinine would then stabilize palladium in the form of the sterically hindered bis-adduct **5** (or possibly the 3:1 adduct).

In an initial experiment $Pd(OAc)_2$ was suspended in toluene and treated with a toluene solution of **1** at $-78\,^{\circ}C$. The color of the solution changed from light orange to deep red within two hours. After 10 h the mixture was warmed to room temperature, and the solvent was removed to provide a red solid, which still contained a small amount of starting material **1** in addition to at least two other phosphorus-containing compounds. Since recrystallization was unsuccessful, the solid residue was redissolved in toluene and chromatographed over Al_2O_3, providing about 60% of a red Pd^0 complex of unknown structure.

The elemental analysis of the red compound indicates the presence of a 2:1 complex PdL_2 ($L = \mathbf{1}$); this is in accord with complex **5**. However, the ^{31}P NMR spectrum displays *two* signals (triplets at $\delta = 179.8$ and 165.5), which clearly shows that the correct structure cannot be as shown. Moreover, the ^1H and ^{13}C NMR spectra are rather complex and are also not in accord with the originally anticipated structure **5**. The speculation that perhaps a dimer is involved was corroborated by mass spectrometry with electro-spray ionization. Thus, the appearance of the protonated mole peak $[M-H]^+$ at 1509 speaks for a dimeric form. Unfortunately, it was not possible to obtain crystals suitable for an X-ray structural analysis, so that the actual structure of the dimer remains unclear.[18]

In hope of obtaining a mono-nuclear complex that might be easier to analyze, the red dimeric complex was treated with triethylphosphane. A dark green powder was isolated in almost quantitative yield. The elemental analysis of the green compound is in the line with $Pd(\mathbf{1})(PEt_3)$ or with an oligomeric species. The ^{31}P NMR spectrum displays two

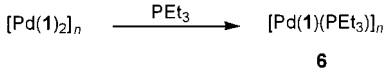

signals at $\delta = 194.6$ and $\delta = 8.3$, which correspond to the phosphorus in the complexed forms of the phosphinine **1** and PEt_3, respectively. However, these and other spectroscopic data did not allow for an unambiguous structural assignment. Fortunately, recrystallization afforded green crystals which turned out to be suitable for an X-ray structural analysis. The results reveal that the compound is a *triangulo* palladium cluster (**6**; $n = 3$), the Pd_3 core being stabilized by two different ligands, namely **1** and PEt_3 (Figure 1). The Pd–Pd bond lengths of 2.819–2.858 Å are in the expected range for *triangulo* palladium cluster, but shorter than those observed in the phosphidobridged tris(μ_2-di-*tert*-butylphosphido-P,P)dicarbonylchloro-tripalladium [average, 2.97(3) Å].[19] Remark-

Abstract in German: *Die Reaktion von $Pd(OAc)_2$ mit 2,4,6-Triphenylphosphinin im Überschuß führt zur Bildung eines roten, dimeren Pd^0-Komplexes unbekannter Struktur. Behandelt man diesen Komplex mit PEt_3, so entsteht ein neuartiger, grüner triangulo-Pd_3-Cluster, der durch drei Phosphinin- und drei PEt_3-Liganden stabilisiert ist. Eine Röntgenstrukturanalyse zeigt, daß die Phosphinin-Liganden als Brücken zwischen je zwei Pd-Atomen dienen. Quantenmechanische Rechnungen an einer Modellverbindung reproduzieren die experimentelle ermittelte Struktur des realen Komplexes recht gut und ermöglichen Aussagen über die Bindungsverhältnisse. So beträgt die Energie der Wechselwirkung zwischen jedem Phosphinin-Liganden und dem Pd_3-Kern 42.2 kcal mol^{-1}, wobei sowohl σ- als auch π-Orbitale beteiligt sind.*

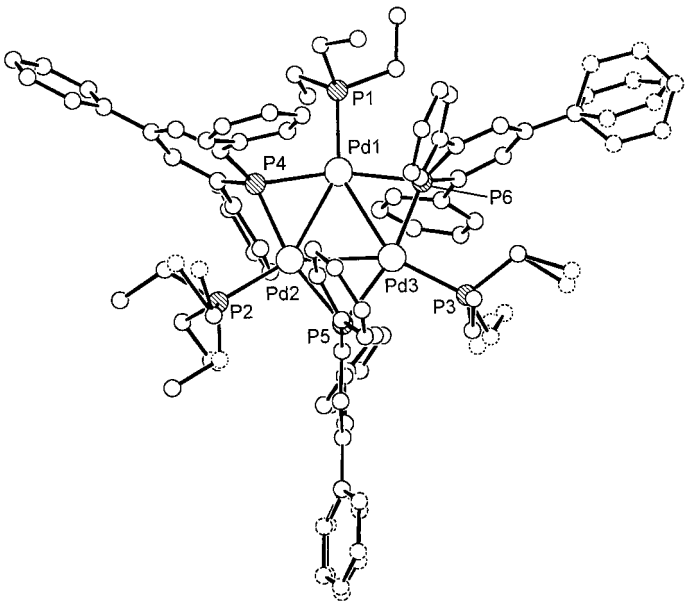

Figure 1. Crystal structure of the tris(μ_2-2,4,6-triphenylphosphinine)-*triangulo*-Pd complex **6** (H atoms and pentane solvent of crystallization removed for clarity; disordered atoms dashed). Selected distances [Å] and angles [°]: Pd1-Pd2 2.8412(5), Pd1-Pd3 2.8581(5), Pd2-Pd3 2.8188(5), Pd1-P1 2.341(1), Pd1-P4 2.331(1), Pd1-P6 2.329(1), Pd2-P2 2.326(1), Pd2-P4 2.336(1), Pd2-P5 2.342(1), Pd3-P3 2.334(1), Pd3-P5 2.327(1), Pd3-P6 2.329(1), Pd1-P4-Pd2 75.02(4), Pd1-P6-Pd3 75.71(4), Pd2-P5-Pd3 74.29(4).

0947-6539/99/0507-2102 $ 17.50+.50/0 *Chem. Eur. J.* **1999**, *5*, No. 7

ably, each phosphinine **1** forms a bridge between two palladium atoms. Such structural features have not been observed previously for Pd_3 clusters nor, as far as we are aware, for a freely coordinated phosphinine ligand.[16]

Quantum-mechanical calculations: In view of the novel structural features of compound **6** ($n=3$), it was of interest to study the electronic nature of the complex. Accordingly, quantum-mechanical calculations were performed on a model compound **7** in which ligand **1** was replaced by the parent phosphinine PC_5H_5 and PEt_3 was replaced by PH_3. Phosphinines themselves, and in some cases metal complexes thereof, have been the subjects of previous theoretical studies.[13, 14] A recent example is the ab initio calculations of the homoleptic tris-(2,2′-biphosphinine) complex of tungsten with six $\eta^1(\sigma)$ bonds.[20] Theoretical calculations have also been reported for the Pd_3 core,[21–23] but not yet for ligand-stabilized *triangulo* Pd_3 clusters.

Technical details of quantum-chemical calculations: Geometry optimizations and single-point energy computations were performed using the Gaussian 94 suite of programs.[24] The Hartree–Fock/density-functional-theory hybrid model B3LYP was applied in combination with the 6-311G(d,p) basis set for phosphorus, carbon, and hydrogen atoms. The 28 chemically inert core electrons of the palladium atoms were replaced by a relativistic pseudopotential,[25] and the valence electrons were described by a [6s5p3d] basis set of valence triple-zeta quality.[25] Population analyses and calculations of Wiberg bond indices[26] were performed with the NBO package[27] as implemented in Gaussian 94. Minor modifications of the Gaussian 94 source code (link 607) were necessary in order to allow for a treatment of more than 500 basis functions by the NBO routines. The analysis of the electron topology according to Bader made use of the program Morphy.[28]

Optimized geometry: In our model (**7**) for the experimentally studied species **6** ($n=3$) we optimized the geometry by employing C_{3h}-symmetry restrictions (Figure 2). Table 1 shows essential bond distances of **7** and the corresponding experimentally determined data.

Considering the model character of **7**, that is, the neglect of the electronic and steric influence of additional groups present in the experimentally employed ligands as well as the lack of symmetry in the crystal structure, the overall agreement between experimental and theoretical data is pleasing. There is a slight overestimation of the computed Pd–Pd and Pd–P bond distances, whereas the calculated P–C

Table 1. Comparison of selected bond lengths [Å] in the Pd_3 core of **7** (Figure 3) computed at the B3LYP level of theory and determined by X-ray crystallography. Owing to the lack of symmetry in the crystal structure, average bond lengths are given. P_μ designates a bridging phosphorus atom, P_{term} a terminal one.

	B3LYP	X-Ray (average)
Pd–Pd	2.884	2.839(20)
Pd–P_{term}	2.353	2.334(8)
Pd–P_μ	2.392	2.332(6)
	2.394	
P_μ–C	1.750	1.764(7)

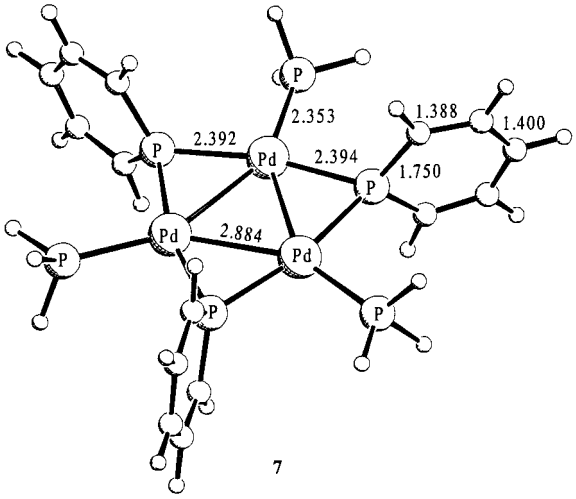

Figure 2. Optimized geometry of **7**. Selected bond lengths are given in Å.

distances in the phosphinine ligands are slightly short. These deviations are probably a consequence of an enhanced donor potential of the real ligands as compared with those used in the model system. In agreement with this supposition, a comparison of the P–C bond length in the coordinated (1.750 Å) and in the free, reoptimized phosphinine (1.743 Å) at the B3LYP level of theory shows that the complexation causes a slight elongation of this bond. Owing to stronger donor/acceptor interactions between the metal core and the ligands, this is more pronounced in the real system. Reoptimization of the isolated Pd_3 fragment in the $^1A'$ singlet state[29] results in a much shorter Pd–Pd bond (2.803 Å in the D_{3h}-symmetric isolated Pd_3 fragment vs. 2.884 Å in **7**); however, the corresponding energy difference between these Pd_3 structures is only 0.3 kcal mol^{-1}. In view of the negligible energetic consequences of an elongation of the Pd–Pd bond, the deviations between computed and experimental bond lengths do not seem significant.

Analysis of bonding properties: In order to understand the intermetallic bonding properties, we first performed calculations on the isolated D_{3h}-symmetric Pd_3 core, using the geometry from **7**. With respect to the dissociation into separated atoms, the Pd_3 cluster is bound by 28.5 kcal mol^{-1}. Relaxation of the geometry does not lead to significant changes, neither in energy nor in electronic structure. It is not immediately apparent how bonding interactions between three Pd atoms in the $4d^{10}5s^0$ ground state could arise. In fact, inspection of the molecular orbitals reveals significant admixture of 5s orbital character to the HOMO – 9, which consists mainly of a $4d_{z^2}/4d_{x^2-y^2}$ hybrid ($c_{|5s\rangle} > 0.1$). This orbital is lowest in energy among the 15 doubly occupied MOs in the valence space of the Pd_3 core. The corresponding antibonding combination of 5s and 4d orbitals forms the LUMO. Significant 5p contributions are not visible in the coefficient vectors of the occupied MOs. A population analysis of the natural orbitals (NPA) of the Pd_3 core yields the electron configuration $4d^{9.86}5s^{0.13}5p^{0.01}$. A Wiberg bond index of 0.24 is calculated for the Pd–Pd bonds, which results in a bond order of 0.48 for each Pd atom. A qualitative MO scheme for the valence orbital space of the Pd_3 core is depicted on the left-

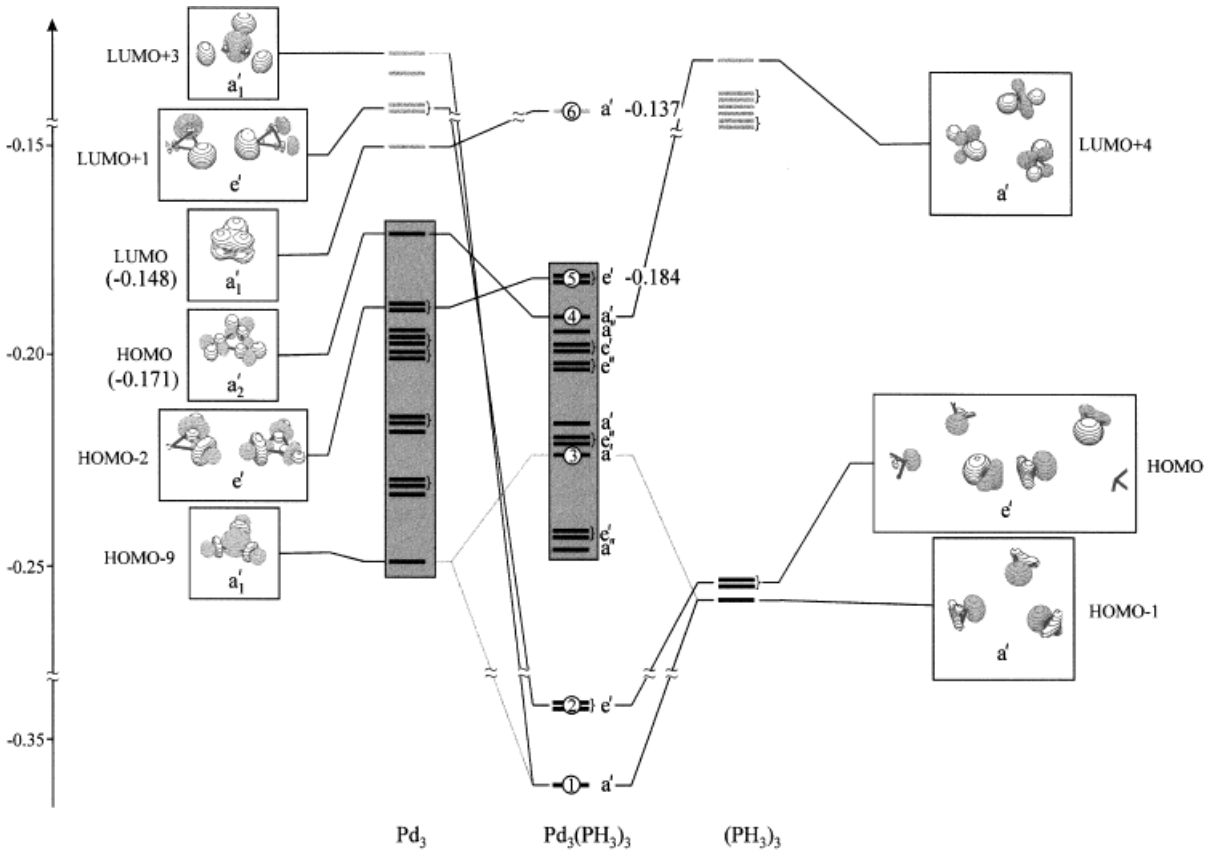

Scheme 1. Orbital interaction scheme for Pd_3 (left) and $(PH_3)_3$ (right) to give the fragment complex $Pd_3(PH_3)_3$.

hand side in Scheme 1. The MO analysis shows that bonding within the isolated Pd_3 cluster is accomplished by formation of occupied 5s/4d hybrid orbitals.

Interactions between the Pd_3 core and the three PH_3 groups were studied by single-point energy calculations on the corresponding C_{3h}-symmetric fragments in the geometry of **7**. These calculations yield an energy of 78.9 kcal mol^{-1} for the formation of the $Pd_3(PH_3)_3$ fragment complex. A highly simplified MO interaction scheme is shown in Scheme 1. Formally, the binding situation can be interpreted in terms of a donation/back-donation picture. The phosphorus lone pairs are interacting with unoccupied orbitals of the metal fragment (donation); this leads to formation of three energetically low-lying bonding orbitals (1 and 2 in Scheme 2). The former HOMO of the Pd_3 fragment is stabilized by an interaction with the LUMO+4 of the symmetry adapted set of $(PH_3)_3$ orbitals and forms the HOMO $-$ 1 of the $Pd_3(PH_3)_3$ complex (back donation, 4 in Scheme 2). In this complex, two e′ orbitals with antibonding character constitute a doubly degenerate HOMO (5 in Scheme 2). The LUMO has s/d hybrid character (6 in Scheme 2), very similar to the LUMO in the isolated Pd_3 fragment.

However, a more detailed analysis of the MOs shows that the bond formation is associated with more complex orbital interactions. For example, the three formal acceptor orbitals of the isolated Pd_3 fragment (LUMO+3 and LUMO+1) possess 5s/5p hybrid character. In contrast, after Pd–P bond formation the MO coefficient vectors of the three lowest valence orbitals (1 and 2 in Scheme 2) do not show significant

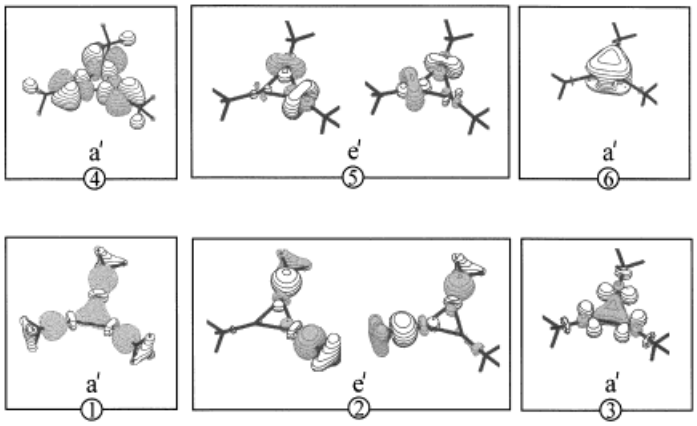

Scheme 2. Selected orbitals essential for bonding in the $Pd_3(PH_3)_3$ fragment complex.

5p character ($c_{|5p\rangle} < 0.02$). In the $Pd_3(PH_3)_3$ complex orbital 1 rather resembles the HOMO $-$ 9 of the Pd_3 core, although $d_{x^2-y^2}$ components are not present and the orbital coefficients localized on the metal show essentially 5s and $4d_{z^2}$ character. Instead, the $d_{x^2-y^2}$ components can now be found in HOMO $-$ 7 (3 in Scheme 2), which shows 4s admixtures and antibonding components of the Pd–P bonds. These interactions are indicated by light gray lines in Scheme 1. A similar situation is found for the equivalent e′-orbital interactions, which are not shown in Scheme 1 for the sake of clarity. Obviously, the promotion of electrons to 5p orbitals of the metal atom is too energy demanding to play any role in the bonding mechanism

  0947-6539/99/0507-2104 $ 17.50+.50/0 *Chem. Eur. J.* **1999**, *5*, No. 7

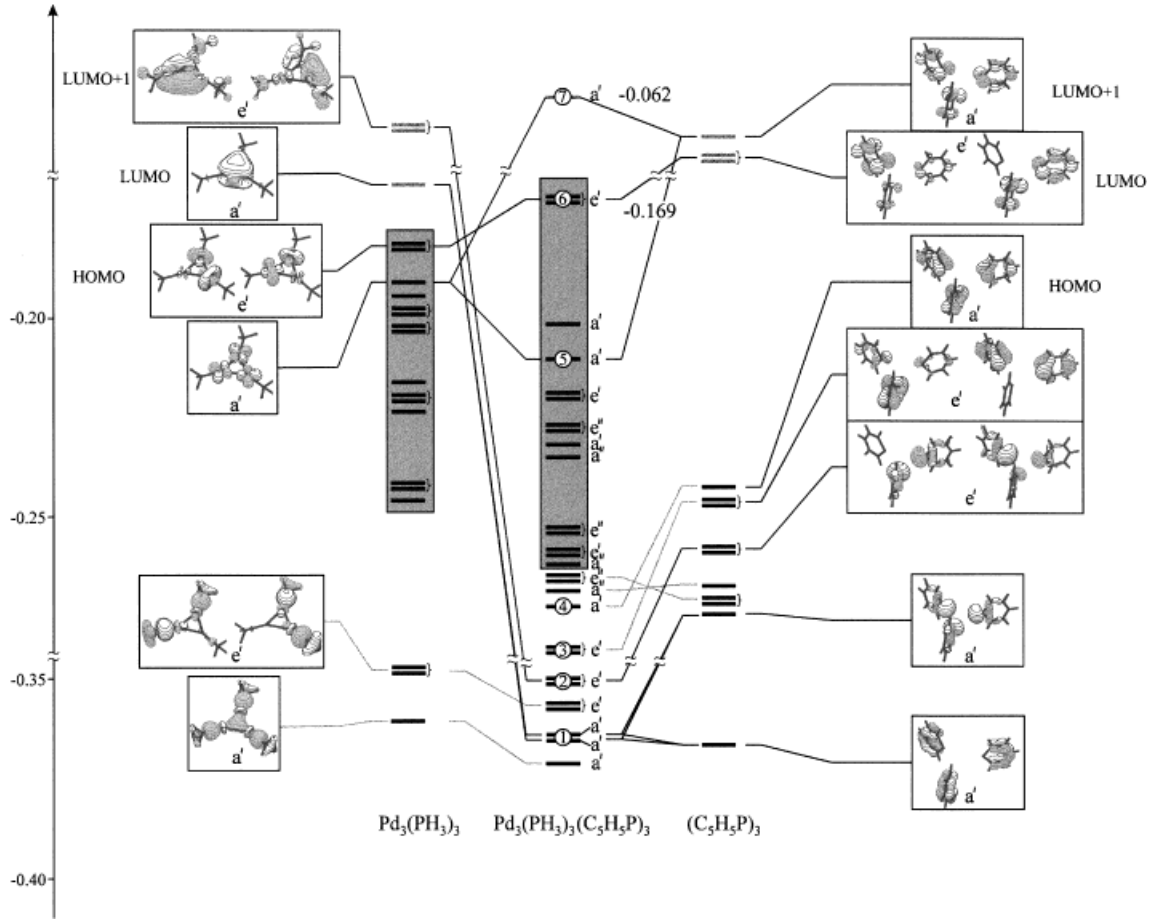

Scheme 3. Orbital interaction scheme for $Pd_3(PH_3)_3$ (left) and $(C_5H_5P)_3$ (right) to give **7**.

of the fragment complex $Pd_3(PH_3)_3$. In agreement, the NPA analysis indicates an electron configuration $4d^{9.80}5s^{0.23}5p^{0.00}$. A Wiberg bond index of 0.10 and 0.41 is calculated for Pd–Pd and Pd–P bonds, respectively; this results in an overall bond order of 0.74 for each Pd atom. In the population analysis, a charge of only -0.03 e is calculated for each Pd atom; this is indicative of an efficient back-bonding mechanism that compensates for the initial transfer of electron density from the PH_3 ligands to the Pd_3 core.

The interactions between the orbitals of $Pd_3(PH_3)_3$ and the $(C_5H_5P)_3$ fragment are complex and only the most important contributions to bonding will be discussed in the following. A simplified picture of the bonding interaction is reproduced in Scheme 3. According to the single point calculations, the three phosphinine ligands are bound by 126.5 kcal mol^{-1}. The HOMO of the free phosphinine ligand has π character, whereas the lone electron pair on phosphorus is only slightly lower in energy. In the $(C_5H_5P)_3$ fragment, these orbitals form C_{3h}-symmetry-adapted linear combinations of a′ and e′ symmetry, which are depicted on the right hand side of Scheme 3. The left-hand side shows the $Pd_3(PH_3)_3$ fragment MOs, which are essential for bonding interactions. As anticipated, the strongest interactions occur between the free σ-electron pairs of the phosphinine ligands and the corresponding unoccupied orbitals of the $Pd_3(PH_3)_3$ fragment [LUMO (a′) and LUMO+1 (e′)]. In addition, lower lying orbitals of the phosphinine ligands with π character are involved, such that two almost degenerate orbitals of a′ symmetry (-0.353 au, -0.354 au, 1 in Scheme 4) are formed, which are very close in energy to the lowest lying valence orbital in the $Pd_3(PH_3)_3$

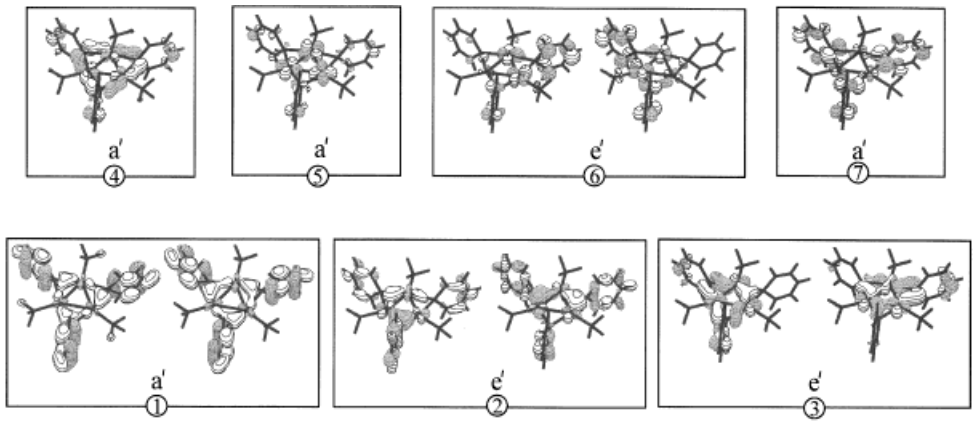

Scheme 4. Selected orbitals essential for bonding in **7**.

fragment (−0.358 au, a′ component of the Pd−P_{term} bond). Very similar interactions lead to the formation of two low-lying bonding orbitals of e′ symmetry (2 in Scheme 4). In addition to these σ-donor interactions of the phosphinine ligands, further analysis of the MOs reveals significant Pd−P_μ contributions with π character to the bonding (3 and 4 in Scheme 4). Stabilizing π interactions occur between the HOMO − 1 (a′) of the $Pd_3(PH_3)_3$ fragment and the LUMO+1 of the phosphinine ligands (back donation, 5 in Scheme 4); the antibonding combination of these MOs forms the LUMO of complex **7** (7 in Scheme 4) and thereby changes its character when compared with the LUMO of the Pd_3 core and the $Pd_3(PH_3)_3$ fragment. The presence of the phosphinine ligands exerts a strongly destabilizing influence on the doubly degenerate HOMO; this is compensated in part by back donation of charge into the doubly degenerate LUMO of the $(C_5H_5P)_3$ fragment. The consequences of these interactions become visible in the graphic representation of orbital 6 in Scheme 4. The population analysis of natural orbitals of **7** yields an electron configuration of $4d^{9.53}5s^{0.47}5p^{0.01}$. The Wiberg bond indices for the respective Pd bonds are: Pd−Pd 0.11, Pd−P_{term} 0.29, and Pd−P_μ 0.35. Altogether, a bond order of 1.58 is computed for each Pd atom. The metal atoms carry a charge of −0.04 e. Again, this indicates the compensation of charge transfer by efficient donation/back-donation mechanisms.

Bader analysis of the electron density: Figure 3 shows the Laplacian of the electron density as well as the bond paths between the metal centers and between metal and phosphorus

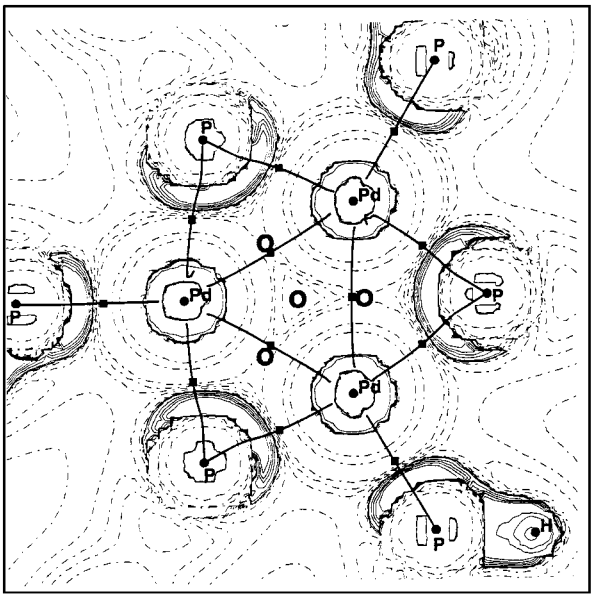

Figure 3. Laplacian of the computed electron density of **7**. Bond paths between Pd and P atoms are shown. Bond critical points are indicated by squares and ring critical points by circles.

atoms. The positions of the bond and ring critical points (marked by squares and circles, respectively) clearly indicate the presence of a Pd_3 ring held together by covalent bonds as well as the covalent nature of the metal–phosphorus bonds. The bridging phosphorus atoms form bonds to two metal atoms and the electron density has ring topology. The representation of the Laplacian shows a significant polarization towards the adjacent Pd atoms in the region of the free electron pairs of the P_μ atoms. This is a consequence of the π-orbital contributions of the phosphinine ligands involved in addition to the σ components of the Pd−P bonding.

Conclusion

The *triangulo* Pd_3 cluster **6** ($n = 3$), in which a phosphinine (**1**) and a phosphane (PEt_3) are involved as ligands, is readily accessible in two steps. The X-ray structural analysis shows novel bonding in that the phosphinine ligands serve as bridges between two Pd atoms. The computed geometry of the model compound **7**, in which the parent substances PC_5H_5 and PH_3 are used as ligands, is in satisfactory agreement with the experimental data. Deviations can be traced back to a very flat stretching potential of the Pd−Pd bonds as well as differences in the donor potential of the ligands in the model and the real system. Interactions between the Pd_3 core and the ligands lead to an overall stabilization energy of 205.4 kcal mol^{-1} (26.3 kcal mol^{-1} per PH_3 group, 42.2 kcal mol^{-1} per C_5H_5P ligand). The analysis of MO interactions shows that the bonding between the phosphinine ligands and the metal core involves both σ and π orbitals. Ligand coordination causes a weakening of the Pd−Pd bonds. This can be understood from the bonding interactions in the isolated Pd_3 fragment; these require an essential admixture of 5s orbital character. If charge is transferred from the ligand lone pairs into these orbitals, they are no longer available for the bond formation between Pd atoms. Consequently, the Pd−Pd bond order is lowered from 0.24 in the Pd_3 fragment to 0.10 in the $Pd_3(PH_3)_3$ fragment or 0.11 in **7**. The presence of efficient back-bonding mechanisms is indicated by negligible charges on the Pd atoms.

Experimental Section

Analytical instrumentation: IR spectra: Magna IR 750 spectrometer (Nicolet). ^1H, ^{31}P, and ^{13}C NMR spectra: FT-NMR AC 200, FT-NMR AM 200, FT-NMR AM 300 and FT-NMR WH 400, all from Bruker; CD_2Cl_2 as internal standard for ^1H and ^{13}C NMR data relative to TMS; ^{31}P NMR shifts relative to 85% H_3PO_4; $\Delta\nu$ = apparent coupling constants from high spin systems; MS: Finnigan MAT 311A, electron spray ionization (ESI-MS) with Finnegan MAT 95. UV/Vis spectra: Cary-2300 spectrometer (Varian). Elemental analyses were carried out by Mikroanalytisches Laboratorium Kolbe, Mülheim an der Ruhr.

Preparation of dimeric complex 5: In a 100 mL Schlenk tube under an atmosphere of argon, a suspension of $Pd(OAc)_2$ (111 mg, 0.5 mmol) in dry toluene (10 mL) was cooled to −78 °C, and a solution of 2,4,6-triphenylphosphinine[13a] (486 mg, 1.5 mmol) in dry toluene (10 mL) was added slowly. Following the addition (1 h) the solution was stirred for an additional 2 h at −78 °C and then for 10 h at room temperature. The solvent was removed in vacuo. The red residue was dissolved in toluene (2 mL) and chromatographed over Al_2O_3 (10 g) with pentane until nonreacted phosphinine **1** was removed; then toluene was used and a fraction which contained the red product. The solvent was stripped off and the product was dried for 24 h under high vacuum; this provided a shiny dark red powder (148 mg corresponding to 60% yield). ^1H NMR (400.14 MHz, CD_2Cl_2): $\delta = 7.84$ (t, $\Delta\nu = 12.2$ Hz, 4H), 7.71 (d, $J = 7.0$ Hz, 4H), 7.70 (t, $\Delta\nu = 15$ Hz, 4H), 7.63 (d, $J = 7.0$), 7.41 (t, $J = 7.7$ Hz, 2H), 7.38

0947-6539/99/0507-2106 $ 17.50+.50/0 *Chem. Eur. J.* **1999**, *5*, No. 7

(t, $J = 7.7$ Hz, 2H), 7.35 (d, $J = 7.7$ Hz, 8H), 7.17 (t, $J = 7.7$ Hz, 4H), 7.13 (m, 8H), 7.11 (m, 8H), 6.92 (m, 4H), 6.90 (m, 8H); ^{13}C NMR (100.62 MHz, CD_2Cl_2): $\delta = 161.89$, 143.15, 158.64, 144.72, 143.22, 142.82, 138.96, 136.88, 133.10, 132.61, 129.28, 129.26, 128.88, 128.19, 127.94, 127.75, 127.70, 127.66, 127.37, 127.22, 127.03, 126.99; ^{31}P NMR: (161.99 MHz, CD_2Cl_2): $\delta = 179.61$ (t, $\Delta\nu = 51$ Hz), 165.28 (pt, $\Delta\nu = 51$ Hz); MS (ESI/pos, CH_2Cl_2): m/z (%): 1509 (60) [M^++H]; IR (KBr): $\tilde{\nu} = 3050$, 3018, 1930–1700, 1596, 1572, 1489, 753, 692 cm^{-1}; UV/Vis (CH_2Cl_2): λ_{max} (ε): 277 (41500), 535 (5500), 677 nm (200); $C_{92}H_{68}P_4Pd_2$ (1510.29): calcd C 73.14, H 4.54, P 8.20, Pd 14.09; found C 71.85, H 4.55, P 7.86, Pd 15.23.

Preparation of compound 6 ($n = 3$): A 100 mL Schlenk tube equipped with a dropping funnel was charged with a solution of dimeric complex **5** (100 mg, 0.07 mmol) in diethyl ether (5 mL) and toluene (2 mL) under an atmosphere of argon. At $-78\,^\circ$C a solution of triethylphosphane (40 mg, 0.34 mmol) in diethyl ether (10 mL) was added slowly; the solution was stirred rapidly throughout. Stirring was continued for 10 h, during which the solution was allowed to warm to room temperature. The solvent was removed, and the dark green residue was dissolved in toluene (1 mL). The solution was covered with a small amount of an ether/pentane (1:1) mixture and allowed to stand for 48 h at $-30\,^\circ$C. A dark green powder precipitated; this was collected and washed 3 times with cold ($-30\,^\circ$C) pentane (3 mL). The product was then dried for 5 h in vacuo (70 mg; 97%). ^{1}H NMR (300.14 MHz, CD_2Cl_2): $\delta = 7.89$ (d, $J = 7.8$ Hz, 8H), 7.68 (m, 4H), 7.52 (d, $J = 7.2$ Hz, 4H), 7.27 (t, $J = 7.6$ Hz, 4H), 7.24 (t, 2H), 6.94 (t, $J = 7.4$ Hz, 4H), 6.74 (t, $J = 7.8$ Hz, 8H), 1.02 (m, 12H), 0.46 (m, 18H); ^{13}C NMR (75.47 MHz, CD_2Cl_2): $\delta = 144.89$ (m), 144.12, 134.70, 129.23, 127.62, 129.12, 125.89, 125.73, 125.82, 16.99, 8.31; ^{31}P NMR (121.50 MHz, CD_2Cl_2): $\delta = 194.61$ (q, $\Delta\nu = 16.0$ Hz), 8.28 (q, $\Delta\nu = 16.0$ Hz); IR (KBr): $\tilde{\nu} = 3040$, 3000, 3055, 3025 (s), 2950 (s), 2929 (s), 1940–1690 (s), 1594, 1566 (m), 1489 (m), 758 (w), 696 cm^{-1} (w); UV/Vis (CH_2Cl_2): λ_{max} (ε): 274 (67400), 330 (36100), 450 (20500), 524 (11600), 689 nm (62700); $C_{58}H_{64}P_4Pd_2$ (1097.88): calcd C 63.55, H 5.88, P 11.28, Pd 19.39; found C 63.58, H 5.81, P 11.24, Pd 19.46.

X-Ray structural analysis of 6: The complex was dissolved in a small amount of toluene, which was then covered with ether/pentane (1:1) at $-30\,^\circ$C. Crystals suitable for an X-ray structural analysis were subsequently obtained on standing. $C_{87}H_{96}P_6Pd_3 \cdot C_5H_{12}$, $M_r = 1718.80$ g mol^{-1}, green, crystal size $0.11 \times 0.25 \times 0.53$ mm, $a = 13.9195(3)$, $b = 17.6501(4)$, $c = 19.9287(4)$ Å, $\alpha = 100.980(1)$, $\beta = 99.024(1)$, $\gamma = 109.917(1)^\circ$, $U = 4386.6(2)$ Å^3, $T = 100$ K, triclinic, $P\bar{1}$ [No. 2], $Z = 2$, $\rho_{calcd} = 1.30$ g cm^{-3}, $\mu = 0.760$ mm^{-1}, Siemens SMART diffractometer, $\lambda = 0.71073$ Å, CCD ω scan, 43317 reflections, of which 23169 were independent, and 18935 considered observed [$I > 2\sigma(I)$], $[(\sin\theta)/\lambda]_{max} = 0.70$ Å^{-1}, spherical absorption correction (T_{min} 0.84526; T_{max} 0.84629), direct methods (SHELXS-97),[30] least-squares refinement[31] (on F_o^2), H atoms riding on nondisordered atoms, disordered atoms isotropic, 891 refined parameters, $R = 0.063$ (obs. data), $R_w = 0.184$ (Chebyshev weights), final shift/error 0.001, residual electron density 1.917 e Å^{-3} (0.923 Å from C90). Crystallographic data (excluding structure factors) for the structures reported in this paper have been deposited with the Cambridge Crystallographic Data Center as supplementary publication no. CCDC-108613. Copies of the data can be obtained free of charge on application to CCDC, 12 Union Road, Cambridge CB2 1EZ, UK (fax: (+44) 1223-336-033; e-mail: deposit@ccdc.cam.ac.uk).

[1] Reviews of transition metal clusters: a) D. Fenske, in *Clusters and Colloids* (Ed.: G. Schmid), VCH, Weinheim, **1994**, chapter 3.4; b) G. Longoni, M. C. Iapalucci, in *Clusters and Colloids* (Ed.: G. Schmid), VCH, Weinheim, **1994**, chapter 3.4; c) P. Braunstein, in *Perspectives in Coordination Chemistry* (Eds.: A. F. Williams, C. Floriani, A. E. Merbach), Helvetica Chimica Acta, Basel, **1992**, pp. 67–107; d) R. J. Puddephatt, L. Manojlovic-Muir, K. W. Muir, *Polyhedron* **1990**, *9*, 2767–2802; e) E. Sappa, A. Tiripicchio, P. Braunstein, *Coord. Chem. Rev.* **1985**, *65*, 219–284; f) N. Zhu, P. Hauser, J. Heinze, H. Vahrenkamp, *J. Cluster Sci.* **1995**, *6*, 147–162; g) G. Süss-Fink, G. Meister, *Adv. Organomet. Chem.* **1993**, *35*, 41–134; h) T. A. Stromnova, I. I. Moiseur, *Russ. Chem. Rev* **1998**, *67*, 485.

[2] Theoretical aspects of transition metal clusters are treated in reviews in ref. [1]; see also: a) N. Rösch, G. Paccioni, in *Clusters and Colloids (Ed.: G. Schmid), VCH, Weinheim,* **1994**, chapter 2; b) J. W. Lauher, *J. Am. Chem. Soc.* **1978**, *100*, 5305–5315; c) D. G. Evans, *J. Organomet. Chem.* **1988**, *352*, 397–413; d) D. J. Underwood, R. Hoffmann, K. Tatsumi, A. Nakamura, Y. Yamamoto, *J. Am. Chem. Soc.* **1985**, *107*, 5968–5980; e) C. Mealli, *J. Am. Chem. Soc.* **1985**, *107*, 2245–2253; f) S. S. M. Ling, N. Hadj-Bagheri, L. Manojlovic-Muir, K. W. Muir, R. J. Puddephatt, *Inorg. Chem.* **1987**, *26*, 231–235; g) F.-W. Cheung, Z. Lin, *Angew. Chem.* **1997**, *109*, 1933–1936; *Angew. Chem. Int. Ed. Engl.* **1997**, *36*, 1847–1849; h) M. L. Buhl, G. J. Long, J. F. O'Brien, *Organometallics* **1993**, *12*, 283–288.

[3] M. Hidai, M. Kokura, Y. Uchida, *J. Organomet. Chem.* **1973**, *52*, 431–435.

[4] C. G. Francis, S. I. Khan, P. R. Morton, *Inorg. Chem.* **1984**, *23*, 3680–3681.

[5] G. W. Bushnell, K. R. Dixon, P. M. Moroney, A. D. Rattray, C. Wan, *J. Chem. Soc. Chem. Commun.* **1977**, 709–710.

[6] A. S. Berenblyum, A. P. Aseeva, L. I. Lakhman, *J. Organomet. Chem.* **1982**, *234*, 237–248.

[7] M. Sommovigo, M. Pasquali, F. Marchetti, P. Leoni, T. Beringhelli, *Inorg. Chem.* **1994**, *33*, 2651–2656.

[8] S. J. Cartwright, K. R. Dixon, A. D. Rattray, *Inorg. Chem.* **1980**, *19*, 1120–1124.

[9] a) K. R. Dixon, A. D. Rattray, *Inorg. Chem.* **1978**, *17*, 1099–1103; b) D. E. Berry, G. W. Bushnell, K. R. Dixon, P. M. Moroney, C. Wan, *Inorg. Chem.* **1985**, *24*, 2625–2634.

[10] A. M. Arif, D. E. Heaton, R. A. Jones, C. M. Nunn, *Inorg. Chem.* **1987**, *26*, 4228–4231.

[11] S. W. Lee, W. C. Trogler, *Inorg. Chem.* **1990**, *29*, 1099–1102.

[12] S. Otsuka, Y. Tatsuno, M. Miki, T. Aoki, M. Matsumoto, H. Yoshioka, K. Nakatsu, *J. Chem. Soc. Chem. Commun.* **1973**, 445–446.

[13] Reviews of the coordination chemistry of phosphinines (λ^3-phosphorins): a) K. Dimroth, *Top. Curr. Chem.* **1973**, *38*, 1–147; b) F. Mathey, *Actual. Chim.* **1996**, *7*, 19–25; c) K. Waschbüsch, P. Le Floch, L. Ricard, F. Mathey, *Chem. Ber./Recl.* **1997**, *130*, 843–849; recent reports: d) P. Le Floch, F. Knoch, F. Kremer, F. Mathey, J. Scholz, W. Scholz, K.-H. Thiele, U. Zenneck, *Eur. J. Inorg. Chem.* **1998**, 119–126; e) N. Avarvari, N. Mézailles, L. Ricard, P. Le Floch, F. Mathey, *Science* **1998**, *280*, 1587–1589; f) P. L. Arnold, F. G. N. Cloke, P. B. Hitchcock, *Chem. Commun.* **1997**, 481–482; g) F. Knoch, F. Kremer, U. Schmidt, U. Zenneck, P. Le Floch, F. Mathey, *Organometallics* **1996**, *15*, 2713–2719; h) B. Breit, R. Winde, K. Harms, *J. Chem. Soc. Perkin Trans. 1* **1997**, 2681–2682; i) H. T. Teunissen, F. Bickelhaupt, *Organometallics* **1996**, *15*, 802–808; j) M. Shiotsuka, T. Tanamachi, Y. Matsuda, *Chem. Lett.* **1995**, 531–532; k) G. Märkl, C. Dörges, T. Riedl, F. G. Klärner, C. Lodwig, *Tetrahedron Lett.* **1990**, *31*, 4589–4592.

[14] C. Elschenbroich, M. Nowotny, A. Behrendt, K. Harms, S. Wocadlo, J. Pebler, *J. Am. Chem. Soc.* **1994**, *116*, 6217–6219.

[15] a) J. Deberitz, H. Nöth, *Chem. Ber.* **1970**, *103*, 2541–2547; b) H. Vahrenkamp, H. Nöth, *Chem. Ber.* **1972**, *105*, 1148–1157; c) H. Vahrenkamp, H. Nöth, *Chem. Ber.* **1973**, *106*, 2227–2235.

[16] 2-(2′-pyridyl)-4,5-dimethylphosphinine ligand μ_2:η^1 bonded to an Ir_2 dimer: B. Schmid, L. M. Venanzi, T. Gerfin, V. Gramlich, F. Mathey, *Inorg. Chem.* **1992**, *31*, 5117–5122; 2-*tert*-butylphosphinine ligand μ_3 bonded to an Os_3 trimer: A. J. Arce, A. J. Deeming, Y. De Sanctis, J. Manzur, *J. Chem. Soc. Chem. Commun.* **1993**, 325–326; 2-trimethylsilylphosphinine ligand μ_3 bonded to an Os_3 trimer: A. J. Arce, A. J. Deeming, Y. De Sanctis, A. M. Garcia, J. Manzur, E. Spodine, *Organometallics* **1994**, *13*, 3381–3383.

[17] E. Bohres, Diplomarbeit, Universität Köln, **1996**.

[18] An Ni^0 complex involving phosphinine **1** and P(*c*-C_6H_{11})$_3$ was reported to be dimeric, but it was not possible to determine its structure: H. Lehmkuhl, R. Paul, R. Mynott, *Liebigs Ann. Chem.* **1981**, 1139–1146. The less bulky parent phosphinine PC_5H_5 forms a well-defined 4:1 $\eta^1(\sigma)$ [$Ni(PC_5H_5)_4$] complex as determined by X-ray crystallography.[14]

[19] A. M. Arif, D. E. Heaton, R. A. Jones, C. M. Nunn, *Inorg. Chem.* **1987**, *26*, 4228–4231.

[20] P. Rosa, L. Ricard, P. Le Floch, F. Mathey, G. Sini, O. Eisenstein, *Inorg. Chem.* **1998**, *37*, 3154–3158.

[21] K. Balasubramanian, *J. Chem. Phys.* **1989**, *91*, 307–313.

[22] M. R. A. Blomberg, P. E. M. Siegbahn, M. Svensson, *J. Phys. Chem.* **1992**, *96*, 5783–5789.

[23] G. Valerio, H. Toulhoat, *J. Phys. Chem.* **1996**, *100*, 10827–10830.

[24] M. J. Frisch, G. W. Trucks, H. B. Schlegel, P. M. W. Gill, B. G. Johnson, M. A. Robb, J. R. Cheeseman, T. Keith, G. A. Petersson, J. A. Montgomery, K. Raghavachari, M. A. Al-Laham, V. G. Zakrzewski, J. V. Ortiz, J. B. Foresman, J. Cioslowski, B. B. Stefanov, A. Nanayakkara, M. Challacombe, C. Y. Peng, P. Y. Ayala, W. Chen, M. W. Wong, J. L. Andres, E. S. Replogle, R. Gomperts, R. L. Martin, D. J. Fox, J. S. Binkley, D. J. Defrees, J. Baker, J. P. Stewart, M. Head-Gordon, C. Gonzalez, J. A. Pople, *Gaussian 94, Revision D.4*, Gaussian, Pittsburgh PA, **1995**.
[25] D. Andrae, U. Haeussermann, M. Dolg, H. Stoll, H. Preuss, *Theor. Chim. Acta* **1990**, *77*, 123 – 141.
[26] K. B. Wiberg, *Tetrahedron* **1968**, *24*, 1083 – 1096.
[27] A. E. Reed, L. A. Curtiss, F. Weinhold, *Chem. Rev.* **1988**, *88*, 899 – 926.
[28] P. L. A. Popelier, *Comput. Phys. Commun.* **1996**, *93*, 212 – 240.
[29] The D_{3h}-symmetric $^1A'$ state of Pd_3 is 9 kcal mol^{-1} higher in energy than the C_{2v}-symmetric $^1A_2$ ground state according to MRCI results.[21] In contrast, a C_{2v}-symmetric $^3B_2$ ground state is found in later work.[22] According to recent B3LYP calculations performed in C_{2v} symmetry, the $^1A_1$ state is higher in energy than the $^3B_2$ ground state by 5.6 kcal mol^{-1}.[23]
[30] G. M. Sheldrick, *Acta Crystallogr. Sect. A* **1990**, *46*, 467 – 473.
[31] G. M. Sheldrick, *SHELXL-97, Program for Crystal Structure Refinement*, Universität Göttingen, **1997**.

Received: November 18, 1998 [F1450]

  0947-6539/99/0507-2108 $ 17.50+.50/0